International Journal of Control, Automation and Systems 16(1) (2018) 1-15
http://dx.doi.org/10.1007/s12555-016-0768-1
ISSN:1598-6446 eISSN:2005-4092
http://www.springer.com/12555

Robust Finite-time Attitude Tracking Control of Rigid Spacecraft Under Actuator Saturation

Hai-Tao Chen, Shen-Min Song*, and Zhi-Bin Zhu

Abstract: This paper investigates the robust finite-time attitude tracking control problem for rigid spacecraft considering the modeling uncertainty, external disturbance and actuator saturation. An auxiliary system is proposed to directly compensate for the saturated control input. First, the basic controller is formulated based on the fast nonsingular terminal sliding mode surface (FNTSMS), the fast-TSM-type reaching law and the auxiliary system in the presence of upper bounded external disturbance. Then, when facing system uncertainty which consists of both modeling uncertainty and external disturbance and has upper bounded first derivative, the extended state observer (ESO) is associated with the first controller to improve the robustness of control system. Furthermore, to handle more general system uncertainty which is upper bounded by a polynomial function of the closed-loop system states, a continuous adaptive controller is designed to compensate for the total system uncertainty on line. The proposed controllers are able to deal with system uncertainty, input singularity and actuator saturation, while simultaneously providing fast finite-time convergence speed for the control system. And the problems of complex parameters selection process and repeated differentiations of nonlinear functions can be avoided. Rigorous stability analyses are given via the Lyapunov stability theory and digital simulations are conducted to illustrate the effectiveness of the proposed controllers.

Keywords: Actuator saturation, adaptive control, auxiliary system, extended state observer (ESO), fast nonsingular terminal sliding mode, fast-TSM-type reaching law.

1. INTRODUCTION

The tracking control problem of rigid spacecraft has attracted much attention due to its importance and wide applications in different kinds of space missions. Many scholars have devoted to the related researches and put forward various methods for the tracking control problem, including the optimal control [1], the passivity-based control [2], the adaptive control [3], the backstepping control [4], the intelligent control [5], the sliding mode control (SMC) [6] and their combinations [7], among which the SMC method has been much favored, due to its easy implementation and active interactions with other control procedures. Especially for the terminal sliding mode control (TSMC) method [8], since it can provide a finite-time convergence rate for the control system, which obtains great advantages in both practical and theoretical situations. Various TSMC-based works with specially defined terminal sliding mode functions have been proposed during the past several decades, such as the conventional terminal sliding mode surface (TSMS) [9, 10], the nonsingular terminal sliding mode surface (NTSMS) [11, 12], the fast terminal sliding mode surface (FTSMS) [13, 14] and the fast nonsingular terminal sliding mode surface (FNTSMS) [15]. This paper is mainly based on the TSMS-based methods to deal with the attitude tracking control problem.

Given the complexity of the spacecraft systems, many factors including the modeling uncertainty, external disturbance and actuator saturation must be considered so that satisfactory control performance can be achieved. The TSMC method possesses strong robustness with respect to the system uncertainty of different types. But many previous works such as [10, 12–15] all require a priori knowledge of the system uncertainty, which may not be available in the actual applications. And the high gain switch functions used to suppress the system uncertainty can cause input chattering and serious actuators worn out. [11] only considers the external disturbance upper bounded by a constant. To off-set the input chattering and to improve the control performance, the observers are combined with the TSMC methods in [16–18] by approximating and com-

Manuscript received December 9, 2016; revised May 11, 2017; accepted June 11, 2017. Recommended by Associate Editor Ohmin Kwon under the direction of Editor Jessie (Ju H.) Park. This paper was supported by the National Natural Science Foundation of China (61174037) and the Foundation for Innovative Research Groups of the National Natural Science Foundation of China (61021002).

Hai-Tao Chen and Shen-Min Song are with the Center for Control Theory and Guidance Technology, Harbin Institute of Technology, Harbin, 150001, China (e-mails: cht2016hit@163.com, songshenmin@hit.edu.cn). Zhi-Bin Zhu is with Beijing Institute of Control Engineering, Beijing, 100190, China (e-mail: zuzijakey@163.com).
* Corresponding author.

pensating for the system uncertainty on line. But the utilization of the observers requires the system uncertainty being differentiable which also restricts the application of the respective controllers. For system uncertainty with more general properties, i.e., being upper bounded by a polynomial function, the adaptive control methods [19–22] are utilized to estimate the respective unknown parameters. Furthermore, when the system uncertainty appears as completely unknown functions, the intelligent algorithms, including the fuzzy logic system [23] and the neural networks [24–27], are able to get real-time approximation of the total uncertainty on line. And with the combination of the adaptive control method, the online computational load of the intelligent methods in [28, 29] can be much reduced because fewer parameters need adjusting. However, [22, 23, 26–29] only provide an asymptotical convergence speed for the closed-loop systems and among all the mentioned TSMC works, only [17, 18] consider the problems of system uncertainty, actuator saturation and finite-time stabilizing concurrently. However, mixing the input errors caused by actuator saturation with modeling uncertainty and external disturbance in [17, 18] would increase the calculation burden of the designed observers and the system dynamic characteristics can be highly affected by the additional disturbance resulting from the saturation effect. Therefore, further research about the attitude tracking control problem considering actuator saturation and system uncertainty is still necessary.

In the existing literatures, the actuator saturation problem has been widely studied. In [30–35], saturation functions are used to formulate the controllers subject to the control input constraints. However, the works of [30–35] involve complex parameter selection processes and can only obtain an asymptotical convergence rate for the closed-loop systems. Homogeneous methods associated with the saturation functions in [36, 37] are able to meet the input saturation constraint and the finite-time stabilizing property, but only when the system uncertainty is absent, which is the main disadvantage of the homogeneous-based control methods. The auxiliary system [38, 39] is a simple but effective method to handle input saturation which includes constructing an extended dynamic system to compensate for the saturated control input in a direct manner. However, the problems exist that in [38] a prior knowledge of the system uncertainty is still necessary and by using neural network to cancel the unknown system uncertainty, the structure of the controller in [39] becomes quite complex. Furthermore, utilizing the conventional backstepping control method in [38, 39] could lead to the problem of explosion of complexity which involves repeated differentiations of nonlinear functions.

As shown above, few existing studies consider the problems of unknown system uncertainty, actuator saturation and input singularity while simultaneously providing a fast finite-time convergence rate for the closed-loop system. Therefore, in this paper three robust control methods are investigated to deal with the above-mentioned problems which are mainly based on the FNTSMS, the auxiliary system, the fast-TSM-type reaching law, the ESO and the adaptive control method. Compared with the existing literatures, contributions of this work include:

1) The fast finite-time convergence rate is obtained considering all the problems of input singularity, input chattering, actuator saturation and unknown system uncertainty.
2) The ESO technique, the fast-TSM-type reaching law and the adaptive control procedure are mainly used to deal with the modeling uncertainty and external disturbance in the proposed controllers, while the auxiliary system is utilized to compensate the actuator saturation effect. Compared with [17, 18], by dealing with the actuator saturation problem and system uncertainty separately, the burden of the respective observers and adaptive laws can be much alleviated and the additional disturbance resulting from the input errors caused by actuator saturation can be much reduced.
3) A modified auxiliary system is proposed so that it could be associated with the FNTSMS, fast-TSM-type reaching law, the ESO and the adaptive control method to handle the actuator saturation, while providing a finite-time convergence rate and robustness against unknown system uncertainty for the control system. In this manner, the problems of complex parameters adjusting process and repeated differentiations of nonlinear functions in the previous works of [30–39] can be avoided.

This paper is organized as follows. Preliminaries and system dynamics are established in the next section. In Section 3, three controllers are proposed and stability proofs are given as well. In Section 4, numerical simulations are presented. The paper is closed with some concluding remarks in Section 5.

2. PROBLEM FORMULATION

Coordinate systems are set up as follows. The inertial frame F_I is centered on the earth center of mass with its x_I axis pointing to the vernal equinox, the z_I axis pointing to the north and parallel to the rotation axis of the earth and the y_I axis given by the right-hand rule. The body fixed frame F_B is centered on the spacecraft center of mass with its axis along with the principle axis of the spacecraft. The reference frame F_R is decided by the desired attitude signal.

According to [40], $q = [q_0 \; q_v^T]^T = [q_0 \; q_1 \; q_2 \; q_3]^T$ is employed to describe the quaternion of the body fixed frame F_B with respect to the inertial frame F_I. The scalar part q_0 and the vector part q_v are subject to the constraint

$q_0^2 + q_v^T q_v = 1$. The attitude dynamics of the spacecraft are defined as (1) and (2).

$$\dot{q} = E(q)\omega, \tag{1}$$

$$J\dot{\omega} = -\omega^{\times} J\omega + u + d, \tag{2}$$

$$E(q) = \begin{bmatrix} -\frac{1}{2}q_v^T \\ \frac{1}{2}(q_0 I_{3\times 3} + q_v^{\times}) \end{bmatrix}, \tag{3}$$

$$x^{\times} = \begin{bmatrix} 0 & -x_3 & x_2 \\ x_3 & 0 & -x_1 \\ -x_2 & x_1 & 0 \end{bmatrix}, \tag{4}$$

where $\omega \in R^{3\times 1}$ is the angular velocity of the spacecraft in the body frame, $J \in R^{3\times 3}$ is the inertia matrix of the spacecraft, $u \in R^{3\times 1}$ and $d \in R^{3\times 1}$ are the control torque and external disturbance torque acting on the spacecraft, respectively. $I_{3\times 3}$ is the 3×3 identity matrix. $x^{\times}$ denotes the skew-symmetric matrix generated by any vector $x = [x_1\ x_2\ x_3]^T \in R^{3\times 1}$.

Denote $q_d = [q_{d0}\ q_{dv}^T]^T$ as the desired attitude of the spacecraft, q_d^* as the conjugate quaternion of q_d and $\omega_d \in R^{3\times 1}$ as the desired angular velocity resolved in the reference frame F_R. Define $\tilde{q}$ and $\tilde{\omega}$ as the error quaternion and error angular velocity of F_B with repect to F_R calculated as

$$\tilde{q} = q_d^* \circ q = [\tilde{q}_0\ \tilde{q}_v^T]^T = [\tilde{q}_0\ \tilde{q}_1\ \tilde{q}_2\ \tilde{q}_3]^T, \tag{5}$$

$$\tilde{\omega} = \omega - C(\tilde{q})\omega_d, \tag{6}$$

where "$\circ$" denotes the multiplication operator between the quaternion. The rotation matrix from F_R to F_B is defined as

$$C = C(\tilde{q}) = (\tilde{q}_0^2 - \tilde{q}_v^T\tilde{q}_v)I_3 + 2\tilde{q}_v\tilde{q}_v^T - 2\tilde{q}_0 q_v^{\times}. \tag{7}$$

Then, it obtains the error dynamics equations:

$$\dot{\tilde{q}} = E(\tilde{q})\tilde{\omega} = \frac{1}{2}\begin{bmatrix} -\tilde{q}_v^T \\ \tilde{q}_0 I_3 + \tilde{q}_v^{\times} \end{bmatrix}\tilde{\omega}, \tag{8}$$

$$J\dot{\tilde{\omega}} = -(\tilde{\omega} + C\omega_d)^{\times} J(\tilde{\omega} + C\omega_d) + J(\tilde{\omega}^{\times} C\omega_d - C\dot{\omega}_d) + \mathrm{sat}(u) + d, \tag{9}$$

$$\mathrm{sat}(u) = [\mathrm{sat}(u_1), \mathrm{sat}(u_2), \mathrm{sat}(u_3)]^T, \tag{10}$$

$$\mathrm{sat}(u_i) = \begin{cases} (U_{\max} - a) + a\tanh(\frac{u_i - U_{\max} + a}{a}) & u_i \geqslant U_{\max} - a, \\ u_i & a - U_{\max} < u_i < U_{\max} - a, \\ (a - U_{\max}) + a\tanh(\frac{u_i + U_{\max} - a}{a}) & u_i \leqslant a - U_{\max}, \end{cases} \tag{11}$$

where $u \in R^{3\times 1}$ is the command control input, $\mathrm{sat}(u) \in R^{3\times 1}$ is the actual saturated control input, $U_{\max}$ is the maximum control torque of the spacecraft on-board actuators, $\tanh(\cdot)$ represents the hyperbolic tangent function, a is a small positive constant chosen by the designer. Given the definition of (11) and using some algebraic operations, it can be proved that, $\mathrm{sat}(u)$ is a piecewise differentiable function with $|u_i| < U_{\max}$ satisfied for $i = 1,2,3$, respectively.

The inertia matrix J can be further described in the form of $J = J_0 + \Delta J$, where J_0 and ΔJ denote a known positive difinite matrix and the unknown modeling uncertainty, respectively. Given the above, (9) becomes

$$\begin{aligned} J_0\dot{\tilde{\omega}} =& -(\tilde{\omega} + C\omega_d)^{\times} J_0(\tilde{\omega} + C\omega_d) \\ &+ J_0(\tilde{\omega}^{\times} C\omega_d - C\dot{\omega}_d) \\ &- (\tilde{\omega} + C\omega_d)^{\times}\Delta J(\tilde{\omega} + C\omega_d) \\ &+ \Delta J(\tilde{\omega}^{\times} C\omega_d - C\dot{\omega}_d) - \Delta J\dot{\tilde{\omega}} + \mathrm{sat}(u) + d \\ =& F + u + \Delta u + \Delta F + d \\ =& F + u + \Delta u + \delta, \end{aligned} \tag{12}$$

$$\begin{aligned} F =& -(\tilde{\omega} + C\omega_d)^{\times} J_0(\tilde{\omega} + C\omega_d) \\ &+ J_0(\tilde{\omega}^{\times} C\omega_d - C\dot{\omega}_d), \end{aligned} \tag{13}$$

$$\begin{aligned} \Delta F =& -(\tilde{\omega} + C\omega_d)^{\times}\Delta J(\tilde{\omega} + C\omega_d) \\ &+ \Delta J(\tilde{\omega}^{\times} C\omega_d - C\dot{\omega}_d) - \Delta J\dot{\tilde{\omega}}, \end{aligned} \tag{14}$$

$$\Delta u = \mathrm{sat}(u) - u, \tag{15}$$

$$\delta = \Delta F + d, \tag{16}$$

where $\delta = [\delta_1\ \delta_2\ \delta_3]^T$ denotes the total system uncertainty.

Property 1: The positive definite matrix J_0 satisfies the following relationship:

$$\lambda_{\min}(J_0)\|x\|_2^2 \leqslant x^T J_0 x \leqslant \lambda_{\max}(J_0)\|x\|_2^2, \forall x \in R^{3\times 1} \tag{17}$$

where $\|\cdot\|_2$ represents the 2-norm of the respective vector or matrix, and $\lambda_{\min}(J_0)$ and $\lambda_{\max}(J_0)$ are the minimum and maximum eigenvalues of J_0, respectively.

Assumption 1 [10, 11, 30]**:** The inertia matrix J, the desired angular velocity ω_d and its derivative $\dot{\omega}_d$ are all assumed to be upper bounded. The external disturbance d is assumed to satisfy $\|d\|_2 < l_1$, where l_1 is an unknown positive constant.

This paper aims at solving the finite-time attitude tracking control problem for rigid spacecraft considering the modeling uncertainty, external disturbance and actuator saturation. The objective is equivalent to designing a command control input u for the attitude tracking control system (8) and (9), so that the finite-time stabilization of the attitude tracking error $\tilde{q}$ (5) and the angular velocity tracking error $\tilde{\omega}$ (6) can be obtained even in the presence of unknown system uncertainty δ (16) and actuator saturation (10).

3. CONTROLLER DESIGN

In this section, the rigid spacecraft attitude tracking control problem is investigated considering system uncertainty and input saturation, with three robust finite-time

saturated control methods proposed. The FNTSMS, the modified auxiliary system and some useful Lemmas are first introduced, which will be useful in the controller formulation and stability analyses sections.

To provide a fast system dynamic and to avoid the input singularity, the FNTSMS is constructed as

$$S = [S_1\ S_2\ S_3]^T = \tilde{\omega} + \alpha_1 \tilde{q}_v + \alpha_2 \beta(\tilde{q}_v), \tag{18}$$

$$\beta(\tilde{q}_v) = [\beta(\tilde{q}_1)\beta(\tilde{q}_2)\beta(\tilde{q}_3)]^T, \tag{19}$$

$$\beta(\tilde{q}_i) = \begin{cases} \mathrm{sig}^{\gamma}(\tilde{q}_i) & |\tilde{q}_i| > \eta, \\ r_1 \tilde{q}_i + r_2\, \mathrm{sgn}(\tilde{q}_i)\tilde{q}_i^2 & |\tilde{q}_i| \leqslant \eta, \end{cases} \tag{20}$$

$$\mathrm{sig}^{\gamma}(\tilde{q}_i) = \mathrm{sgn}(\tilde{q}_i)|\tilde{q}_i|^{\gamma}, \tag{21}$$

$$\mathrm{sgn}(\tilde{q}_i) = \begin{cases} 1 & \tilde{q}_i > 0, \\ 0 & \tilde{q}_i = 0, \\ -1 & \tilde{q}_i < 0, \end{cases} \tag{22}$$

where $r_1 = (2-\gamma)\eta^{\gamma-1}$, $r_2 = (\gamma-1)\eta^{\gamma-2}$, $0 < \gamma, \eta < 1$ and $i = 1,2,3$.

The auxiliary system to compensate for the actuator saturation is designed as follows:

$$\dot{\zeta} = \begin{cases} 0, & \|\zeta\|_2 \leqslant \zeta_0, \\ -k_1\zeta - k_2 \mathrm{sig}^{\gamma_1}(\zeta) - \dfrac{\|S^T\Delta u\|_1 + 0.5\Delta u^T\Delta u}{\|\zeta\|_2^2}\zeta + \Delta u, & \|\zeta\|_2 > \zeta_0, \end{cases} \tag{23}$$

where Δu is as defined in (15), $\zeta \in R^{3\times 1}$ is the state vector, $S \in R^{3\times 1}$ is as defined in (18), k_1, k_2 and ζ_0 are positive constants chosen by the designer, $\mathrm{sig}^{\gamma_1}(\zeta) = [\mathrm{sig}^{\gamma_1}(\zeta_1), \mathrm{sig}^{\gamma_1}(\zeta_2), \mathrm{sig}^{\gamma_1}(\zeta_3)]^T$ and $0 < \gamma_1 < 1$.

Lemma 1 [11]**:** Suppose $a_1 > 0$, $a_2 > 0$ and $0 < c < 1$. Then, it obtains

$$(a_1 + a_2)^c \leqslant a_1^c + a_2^c. \tag{24}$$

Lemma 2 [11]**:** Suppose $a_1 > 0, \ldots, a_n > 0$ and $0 < c < 2$. Then, it obtains

$$(a_1^2 + a_2^2 + \cdots + a_n^2)^c \leqslant (a_1^c + a_2^c + \cdots + a_n^c)^2. \tag{25}$$

Lemma 3 [10]**:** For $y = f(x)$, $x \in R^{n\times 1}$ and $f(0) = 0$. Suppose that $V(x)$ is a C^1 smooth positive definite function (defined on $U \subset R^{n\times 1}$) and $\dot{V}(x) + aV(x)^c$ is a negative semi-definite function defined on $U \subset R^{n\times 1}$ where $a > 0$ and $0 < c < 1$. Then, there exist $U_0 \subset R^{n\times 1}$ so that any $V(x)$ that starts from $U_0 \subset R^{n\times 1}$ can reach $V(x) \equiv 0$ in finite time. If T is the time for $V(x) \equiv 0$ to be reached,

$$T \leqslant \frac{V(x(t_0))^{1-c}}{a(1-c)}, \tag{26}$$

where $V(x(t_0))$ is the initial value of $V(x)$. Then, $y = f(x)$ is finite-time stable.

Lemma 4 [10]**:** For $y = f(x)$, $x \in R^{n\times 1}$ and $f(0) = 0$. If $V(x)$ which is defined in Lemma 3 satisfies $\dot{V}(x) \leqslant -aV(x) - bV(x)^c$, where $a > 0$, $b > 0$ and $0 < c < 1$. Then, $V(x) \equiv 0$ can be reached after

$$T \leqslant \frac{1}{a(1-c)} \ln \frac{aV(x(t_0))^{1-c} + b}{b}. \tag{27}$$

Lemma 5 [14, 21]**:** Consider the systems (8) and (9) and S (18). If $S = 0$ is achieved, $\tilde{q}$ and $\tilde{\omega}$ can first converge into small regions around the expected equilibrium of $\{\tilde{q} = [1, 0_{3\times 1}]^T, \tilde{\omega} = 0\}$ in finite time and then to the expected equilibrium as time tends to infinity.

Proof: The equilibriums of the systems (8) and (9) are $\{\tilde{q} = [\pm 1, 0_{3\times 1}]^T, \tilde{\omega} = 0\}$.Using $S = 0$ yields

$$\tilde{\omega} + \alpha_1 \tilde{q}_v + \alpha_2 \beta(\tilde{q}_v) = 0. \tag{28}$$

For $\{\tilde{q} = [-1, 0_{3\times 1}]^T, \tilde{\omega} = 0\}$, the Lyapunov candidate function is designed as

$$V_1 = \tilde{q}_v^T \tilde{q}_v + (1 + \tilde{q}_0)^2. \tag{29}$$

Taking the derivative of (29),

$$\dot{V}_1 = \alpha_1 \tilde{q}_v^T \tilde{q}_v + \alpha_2 \tilde{q}_v^T \beta(\tilde{q}_v) > 0. \tag{30}$$

Hence, $\{\tilde{q} = [-1, 0_{3\times 1}]^T, \tilde{\omega} = 0\}$ is unstable and any small disturbance can make the system leave $\{\tilde{q} = [-1, 0_{3\times 1}]^T, \tilde{\omega} = 0\}$.

For $\{\tilde{q} = [1, 0_{3\times 1}]^T, \tilde{\omega} = 0\}$, define

$$V_2 = \tilde{q}_v^T \tilde{q}_v + (1 - \tilde{q}_0)^2. \tag{31}$$

Taking the derivative of (31),

$$\dot{V}_2 = -\alpha_1 \tilde{q}_v^T \tilde{q}_v - \alpha_2 \tilde{q}_v^T \beta(\tilde{q}_v). \tag{32}$$

When $|\tilde{q}_i| > \eta$, the system is obtained that

$$\begin{aligned} \dot{V}_2 &\leqslant -\alpha_1 \tilde{q}_v^T \tilde{q}_v - \alpha_2 (\tilde{q}_v^T \tilde{q}_v)^{\frac{\gamma+1}{2}} \\ &\leqslant -\frac{1}{2}\alpha_1 \cdot (2\tilde{q}_v^T \tilde{q}_v) - (\frac{1}{2})^{\frac{\gamma+1}{2}} \alpha_2 \cdot (2\tilde{q}_v^T \tilde{q}_v)^{\frac{\gamma+1}{2}} < 0. \end{aligned} \tag{33}$$

Hence, $\{\tilde{q} = [1, 0_{3\times 1}]^T, \tilde{\omega} = 0\}$ is a stable equilibrium and $\tilde{q}_0 \geqslant 0$ can be reached after finite time. Then,

$$(1 - \tilde{q}_0)^2 - q_v^T q_v = 2\tilde{q}_0(\tilde{q}_0 - 1) \leqslant 0. \tag{34}$$

Using (31) and (34),

$$V_2 \leqslant 2\tilde{q}_v^T \tilde{q}_v, \tag{35}$$

$$\dot{V}_2 \leqslant -\frac{1}{2}\alpha_1 \cdot V_2 - (\frac{1}{2})^{\frac{\gamma+1}{2}} \alpha_2 \cdot V_2^{\frac{\gamma+1}{2}}. \tag{36}$$

Based on Lemma 4, $|\tilde{q}_i| \leqslant \eta$ can be reached in finite time, which is the same with $\tilde{\omega}$ and the ultimate upper bound of $\tilde{\omega}$ is decided by:

$$|\tilde{\omega}_i| \leqslant \alpha_1 |\tilde{q}_i| + \alpha_2 |\tilde{q}_i|^{\gamma} \leqslant \alpha_1 \eta + \alpha_2 \eta^{\gamma}, i = 1,2,3. \tag{37}$$

And the time consumption T for the reach of $|\tilde{q}_i| \leqslant \eta$ can be estimated as:

$$T \leqslant \frac{4}{\alpha_1(1-\gamma)} \ln \frac{2^{\frac{\gamma-1}{2}} V_2(t_0)^{\frac{1-\gamma}{2}} + \alpha_2}{\alpha_2}, \tag{38}$$

where t_0 is the time when $\tilde{q}_0 \geqslant 0$ is reached.

When $|\tilde{q}_i| \leqslant \eta$,

$$\begin{aligned} \dot{V}_2 &= -\frac{1}{2}(\alpha_1 + \alpha_2 r) \cdot (2\tilde{q}_v^T \tilde{q}_v) - \alpha_2 r_2 \sum_{i=1}^{3} (|\tilde{q}_i| \cdot \tilde{q}_i^2) \\ &\leqslant -\frac{1}{2}(\alpha_1 + \alpha_2 r) \cdot V_2. \end{aligned} \tag{39}$$

Therefore, $\tilde{q}_v = 0$ can be reached as time tends to infinity, which also applies to $\tilde{\omega}$ because of $S = 0$.

The completes the proof of Lemma 5. □

3.1. The basic finite-time saturated attitude tracking controller design

In this subsection, the external disturbance and actuator saturation are considered and the modeling uncertainty of ΔJ is neglected, i.e., $\Delta J = 0$, $\Delta F = 0$ and $\delta = d$. To handle the external disturbance as stated in Assumption 1 and the actuator saturation effect as defined in (10), and to provide finite-time convergence rate for the closed-loop system, the fast-TSM-type reaching law is associated with the FNTSMS (18) and the auxiliary system (23) to formulate the controller.

The command control signal u is designed as

$$\begin{aligned} u &= -F - \alpha_1 J_0 \dot{\tilde{q}}_v - \alpha_2 J_0 \dot{\beta}(\tilde{q}_v) - k_3 \zeta - \frac{1}{2} S \\ &\quad + u_r + u_n, \end{aligned} \tag{40}$$

$$u_r = -\tau_1 S - \tau_2 \mathrm{sig}^{\rho}(S), \tag{41}$$

$$u_n = -k_4 \mathrm{sig}^{\gamma_1}(S), \tag{42}$$

$$k_1 - \frac{1}{2}k_3^2 - \frac{1}{2} > 0, \tag{43}$$

where $0 < \rho, \gamma_1 < 1$, α_1 and α_2 are as defined in (18), τ_1, τ_2, k_3 and k_4 are positive constants, and k_1 is as defined in (23).

Then, it obtains the following theorem.

Theorem 1: Consider the systems in (8) and (9). If Assumption 1 holds, the modeling uncertainty is neglected, the auxiliary system is designed as (23) and the controller (40) is applied. Then, the following conclusions are obtained:

(i) The sliding mode surface $S = [S_1\ S_2\ S_3]^T$ can converge into the following regions in finite time:

$$|S_i| \leqslant \phi_i = \min\{\frac{|d_i|}{\tau_1}, \left|\frac{d_i}{\tau_2}\right|^{\frac{1}{\rho}}\}, i = 1,2,3, \tag{44}$$

where $|d_i|$ is the absolute value of the i^{th} element of the external disturbance d, and τ_1, τ_2 and ρ are as defined in (41).

(ii) The tracking errors of $\tilde{q}_v$ and $\tilde{\omega}$ can converge into the following regions in finite time:

$$|\tilde{q}_i| \leqslant Q_i = \max\{\eta, \min\{\frac{|\phi_i|}{\alpha_1}, \left|\frac{\phi_i}{\alpha_2}\right|^{\frac{1}{\gamma}}\}\}, \tag{45}$$

$$|\tilde{\omega}_i| \leqslant \phi_i + \alpha_1 Q_i + \alpha_2 Q_i^{\gamma}, i = 1,2,3, \tag{46}$$

where ϕ_i is as defined in (44), and η, α_1, α_2 and γ are as defined in (18) and (20).

Proof: Consider the Lyapunov candidate function as

$$V = \frac{1}{2} S^T J_0 S + \frac{1}{2} \zeta^T \zeta. \tag{47}$$

Taking the derivative of (47) and substituting in the controller (40) and the auxiliary system (23) yields

$$\begin{aligned} \dot{V} &= S^T [F + u + \Delta u + d + \alpha_1 J_0 \dot{\tilde{q}}_v + \alpha_2 J_0 \dot{\beta}(\tilde{q}_v)] \\ &\quad + \zeta^T \dot{\zeta} \\ &= S^T (d + u_r - k_4 \cdot \mathrm{sig}^{\gamma_1}(S) - k_3 \zeta - \frac{1}{2} S + \Delta u) \\ &\quad + \zeta^T \dot{\zeta} \\ &= S^T (d + u_r) - k_4 \cdot S^T \mathrm{sig}^{\gamma_1}(S) - k_3 S^T \zeta - \frac{1}{2} S^T S \\ &\quad + S^T \Delta u - k_1 \zeta^T \zeta - k_2 \zeta^T \mathrm{sig}^{\gamma_1}(\zeta) - \left\| S^T \Delta u \right\|_1 \\ &\quad - \frac{1}{2} \Delta u^T \Delta u + \zeta^T \Delta u. \end{aligned} \tag{48}$$

Using the inequalities of $-k_3 S^T \zeta \leqslant \frac{1}{2} S^T S + \frac{1}{2} k_3^2 \zeta^T \zeta$ and $\zeta^T \Delta u \leqslant \frac{1}{2} \zeta^T \zeta + \frac{1}{2} \Delta u^T \Delta u$,

$$\begin{aligned} \dot{V} &\leqslant -k_4 S^T \mathrm{sig}^{\gamma_1}(S) - k_2 \zeta^T \mathrm{sig}^{\gamma_1}(\zeta) \\ &\quad - \zeta^T (k_1 - \frac{1}{2} k_3^2 - \frac{1}{2}) \zeta + S^T (d + u_r) \\ &\leqslant -k_4 (S^T S)^{\frac{\gamma_1+1}{2}} - k_2 (\zeta^T \zeta)^{\frac{\gamma_1+1}{2}} \\ &\quad - \zeta^T (k_1 - \frac{1}{2} k_3^2 - \frac{1}{2}) \zeta + S^T (d + u_r). \end{aligned} \tag{49}$$

Using (43),

$$\begin{aligned} \dot{V} &\leqslant -(\frac{2}{\lambda_{\max}(J_0)})^{\frac{\gamma_1+1}{2}} k_4 (\frac{1}{2} S^T J_0 S)^{\frac{\gamma_1+1}{2}} \\ &\quad - 2^{\frac{\gamma_1+1}{2}} k_2 (\frac{1}{2} \zeta^T \zeta)^{\frac{\gamma_1+1}{2}} + S^T (d + u_r) \\ &\leqslant -\mu \cdot V^{\frac{\gamma_1+1}{2}} + S^T (d - \tau_1 S - \tau_2 \mathrm{sig}^{\rho}(S)), \end{aligned} \tag{50}$$

where $\mu = \min((2/\lambda_{\max}(J_0)))^{(\gamma_1+1)/2} \cdot k_4, 2^{(\gamma_1+1)/2} \cdot k_2)$.

Equation (50) can be rewritten as:

$$\begin{aligned} \dot{V} &\leqslant -\mu \cdot V^{\frac{\gamma_1+1}{2}} - \\ &\quad S^T [\mathrm{diag}(\tau_1 - \frac{d_i}{S_i}) S + \tau_2 \mathrm{sig}^{\rho}(S)], \end{aligned} \tag{51}$$

$$\begin{aligned} \dot{V} &\leqslant -\mu \cdot V^{\frac{\gamma_1+1}{2}} - \\ &\quad S^T [\tau_1 S + diag(\tau_2 - \frac{d_i}{\mathrm{sgn}(S_i)|S_i|^{\rho}}) \mathrm{sig}^{\rho}(S)], \end{aligned} \tag{52}$$

where $\mathrm{diag}(x_i)$ represents a diagonal matrix with the diagonal elements of x_i $(i=1,2,3)$.

If $\tau_1 > |d_i|/|S_i|$ or $\tau_2 > |d_i|/|S_i|^\rho$ are satisfied for $i=1,2,3$, respectively, $\mathrm{diag}(\tau_1 - d_i/S_i)$ or $\mathrm{diag}(\tau_2 - d_i/\mathrm{sgn}(S_i)|S_i|^\rho)$ can be kept positive definite.

Then, the system becomes

$$\dot{V} \leqslant -\mu V^{\frac{\gamma_1+1}{2}}. \tag{53}$$

Using Lemma 2, the convergence of the attitude tracking control system can be assured until $\tau_1 \leqslant |d_i|/|S_i|$ and $\tau_2 \leqslant |d_i|/|S_i|^\rho$ have all been reached. Therefore, S can converge into the following regions in finite time:

$$|S_i| \leqslant \phi_i = \min\{\frac{|d_i|}{\tau_1}, \left|\frac{d_i}{\tau_2}\right|^{\frac{1}{\rho}}\}, i=1,2,3, \tag{54}$$

where τ_1, τ_2 and ρ are as defined in (41).

Now (i) has been proven.

(ii) The stability analysis of $\tilde{q}_i$ and $\tilde{\omega}_i$ $(i=1,2,3)$ should be divided into the following two cases:

When $|\tilde{q}_i| \leqslant \eta$, it yields

$$\tilde{\omega}_i + \alpha_1\tilde{q}_i + \alpha_2(r_1\tilde{q}_i + r_2\,\mathrm{sgn}(\tilde{q}_i)\tilde{q}_i^2) = S_i. \tag{55}$$

which can be rewritten as

$$\tilde{\omega}_i + (\alpha_1 - \frac{S_i}{\tilde{q}_i})\tilde{q}_i + \alpha_2(r_1\tilde{q}_i + r_2\,\mathrm{sgn}(\tilde{q}_i)\tilde{q}_i^2) = 0, \tag{56}$$

$$\begin{aligned}&\tilde{\omega}_i + \alpha_1\tilde{q}_i + (\alpha_2 - \frac{S_i}{r_1\tilde{q}_i + r_2\,\mathrm{sgn}(\tilde{q}_i)\tilde{q}_i^2})\\ &\times (r_1\tilde{q}_i + r_2\,\mathrm{sgn}(\tilde{q}_i)\tilde{q}_i^2) = 0.\end{aligned} \tag{57}$$

If $\alpha_1 > |S_i|/|\tilde{q}_i|$ or $\alpha_2 > |S_i|/\left|r_1\tilde{q}_i + r_2\,\mathrm{sgn}(\tilde{q}_i)\tilde{q}_i^2\right|$ can be assured, (56) or (57) become a linear SMS and the convergence of $\tilde{q}_v$ and $\tilde{\omega}$ is assured. Furthermore,

$$\begin{aligned}&\left|r_1\tilde{q}_i + r_2\,\mathrm{sgn}(\tilde{q}_i)\tilde{q}_i^2\right|\\ &\leqslant \left|(2-\gamma)\eta^{\gamma-1}\tilde{q}_i\right| + \left|(\gamma-1)\eta^{\gamma-2}\,\mathrm{sgn}(\tilde{q}_i)\tilde{q}_i^2\right|\\ &\leqslant (\frac{2}{\eta^{1-\gamma}} + \frac{1}{\eta^{2-\gamma}})\,|\tilde{q}_i|.\end{aligned} \tag{58}$$

$\alpha_1 > |S_i|/|\tilde{q}_i|$ and $\alpha_2 > |S_i|/\left|r_1\tilde{q}_i + r_2\,\mathrm{sgn}(\tilde{q}_i)\tilde{q}_i^2\right|$ yield $|\tilde{q}_i| > |S_i|/\alpha_1$ and $|\tilde{q}_i| > (\frac{2}{\eta^{1-\gamma}} + \frac{1}{\eta^{2-\gamma}})^{-1}\cdot|S_i|/\alpha_2$. Based on $|S_i| \leqslant \phi_i$, $|\tilde{q}_i| \leqslant \eta$ and Lemma 5, $\tilde{q}_v$ and $\tilde{\omega}$ can converge into the following regions in finite time:

$$|\tilde{q}_i| \leqslant Q_{1i} = \min\{\eta, \frac{|\phi_i|}{\alpha_1}, (\frac{2}{\eta^{1-\gamma}} + \frac{1}{\eta^{2-\gamma}})^{-1}\cdot\frac{|\phi_i|}{\alpha_2}\}, \tag{59}$$

$$\begin{aligned}|\tilde{\omega}_i| &\leqslant |S_i| + \alpha_1\,|\tilde{q}_i| + \alpha_2(\frac{2}{\eta^{1-\gamma}} + \frac{1}{\eta^{2-\gamma}})\,|\tilde{q}_i|\\ &\leqslant \phi_i + \alpha_1 Q_{1i} + \alpha_2(\frac{2}{\eta^{1-\gamma}} + \frac{1}{\eta^{2-\gamma}})Q_{1i},\end{aligned} \tag{60}$$

where ϕ_i is as defined in (54), and α_1, α_2, γ and η are as defined in (18) and (20).

When $|\tilde{q}_i| > \eta$, it yields

$$\tilde{\omega}_i + \alpha_1\tilde{q}_i + \alpha_2\,\mathrm{sgn}(\tilde{q}_i)|\tilde{q}_i|^\gamma = S_i. \tag{61}$$

Equation (61) can be rewritten as

$$\tilde{\omega}_i + (\alpha_1 - \frac{S_i}{\tilde{q}_i})\tilde{q}_i + \alpha_2\,\mathrm{sgn}(\tilde{q}_i)|\tilde{q}_i|^\gamma = 0, \tag{62}$$

$$\tilde{\omega}_i + \alpha_1\tilde{q}_i + (\alpha_2 - \frac{S_i}{\mathrm{sgn}(\tilde{q}_i)|\tilde{q}_i|^\gamma})\,\mathrm{sgn}(\tilde{q}_i)|\tilde{q}_i|^\gamma = 0. \tag{63}$$

If $\alpha_1 > |S_i|/|\tilde{q}_i|$ or $\alpha_2 > |S_i|/|\tilde{q}_i|^\gamma$ is satisfied, (62) or (63) become a classical FTSMS. Then, the convergence of $\tilde{q}_v$ and $\tilde{\omega}$ can be assured until $|\tilde{q}_i| \leqslant |S_i|/\alpha_1$ and $|\tilde{q}_i|^\gamma \leqslant |S_i|/\alpha_2$ are all reached. Using $|S_i| \leqslant \phi_i$, $|\tilde{q}_i| > \eta$ and Lemma 5, the following regions can be reached in finite time:

$$|\tilde{q}_i| \leqslant Q_{2i} = \max\{\eta, \min\{\frac{|\phi_i|}{\alpha_1}, \left|\frac{\phi_i}{\alpha_2}\right|^{\frac{1}{\gamma}}\}\}, \tag{64}$$

$$|\tilde{\omega}_i| \leqslant |S_i| + \alpha_1\,|\tilde{q}_i| + \alpha_2|\tilde{q}_i|^\gamma \leqslant \phi_i + \alpha_1 Q_{2i} + \alpha_2 Q_{2i}^\gamma, \tag{65}$$

where ϕ_i is as defined in (54), and α_1, α_2, γ and η are as defined in (18) and (20).

Therefore, the ultimate upper bounds of $\tilde{q}_v$ and $\tilde{\omega}$ should be given as (64) and (65).

Now (ii) has been proven.

The proof of Theorem 1 is complete. □

Remark 1: With the addition of $-k_2\mathrm{sig}^{\gamma_1}(\zeta)$, it becomes possible to directly associate the auxiliary system with FNTSMS to handle the actuator saturation problem and to provide a finite-time convergence rate for the control system. In this manner, the complex parameters adjusting process in [30–35] are no longer necessary and the problem of "complexity explosion" in [38,39] can also be avoided.

Remark 2: The ultimate upper bounds of the tracking errors as stated in (64) and (65) are able to cover both the cases of $|\tilde{q}_i| \leqslant \eta$ and $|\tilde{q}_i| > \eta$ $(i=1,2,3)$. However, when $|\tilde{q}_i| \leqslant \eta$ has been reached, a less conservative and more useful result about the steady states precisions should be decided by (59) and (60). Similar results can be derived for Theorems 2 and 3.

Remark 3: From (54), (64) and (65), it can be seen that, the steady states accuracy is highly affected by the amplitude of the system uncertainty. If the system uncertainty acting on the spacecraft can be counteracted to a large extent, the control precision would get much increased. The ESO technique has been an active method to improve the robustness of the control system. Besides, by using ESO to estimate and compensate for the system uncertainty on line, not only the control precision can get improved, but also the input chattering problem in the traditional TSMC-based control works [10,14] can be much attenuated, especially when the system uncertainty is differentiable and has upper bounded first derivative.

3.2. The ESO-based finite-time saturated attitude tracking controller design

In this subsection, to further improve the control precision of the controller (40) in Theorem 1, the ESO is designed to associate with the FNTSMS (18), the auxiliary system (23) and the fast-TSM-type reaching law to formulate the attitude tracking controller. To facilitate the utilization of the ESO, the following assumption is first introduced.

Assumption 2 [18,41]**:** The total system uncertainty δ as defined in (16) is differentiable and has upper bounded first derivative.

Remark 4: δ contains both the external disturbance and the modeling uncertainty. Assumption 2 implies that the external disturbance, the modeling uncertainty and their combinations are all differentiable and have upper bounded first derivative. It is based on the consideration that when the spacecraft systems are under control, the control torques may vary with time, but the change rate of the control torques, together with the modeling parameters can not be infinite in reality. Though conservative, it can still cover many practical situations, as stated in [18,41]. Therefore, it is reasonable to have Assumption 2 in this subsection.

The ESO system is designed on the basis of (12) which is rewritten as:

$$\dot{\tilde{\omega}} = J_0^{-1}F + J_0^{-1}\,\mathrm{sat}(u) + x_2, \tag{66}$$

$$\dot{x}_2 = f(t), \tag{67}$$

where $x_2 = J_0^{-1}\delta$ and $f(t)$ is the derivative of x_2. According to Assumption 2, $f(t)$ is upper bounded. $J_0^{-1}\delta$ is the extended state to be estimated.

The second-order ESO [18] is constructed as follows:

$$e_1 = [e_{11}e_{12}e_{13}]^T = Z_1 - \tilde{\omega}, \tag{68}$$

$$\dot{Z}_1 = Z_2 + J_0^{-1}F + J_0^{-1}\,\mathrm{sat}(u) - z_1 e_1, \tag{69}$$

$$\dot{Z}_2 = -z_2 f(e_1, \alpha_0, \varepsilon_0) \tag{70}$$

where

$$f(e_1,\alpha_0,\varepsilon_0) = [f_1(e_1,\alpha_0,\varepsilon_0) \quad f_2(e_1,\alpha_0,\varepsilon_0) \quad f_3(e_1,\alpha_0,\varepsilon_0)]^T, \tag{71}$$

$$f(e_i,\alpha_0,\varepsilon_0) = \begin{cases} \mathrm{sig}^{\alpha_0}(e_{1i}) & |e_{1i}| > \varepsilon_0 \\ e_{1i}/\varepsilon_0^{1-\alpha_0} & |e_{1i}| \leqslant \varepsilon_0 \end{cases}, \tag{72}$$

$$0 < \alpha_0, \varepsilon_0 < 1, \tag{73}$$

$$\mathrm{sig}^{\alpha_0}(e_{1i}) = \mathrm{sgn}(e_{1i})|e_{1i}|^{\alpha_0}, i = 1,2,3, \tag{74}$$

and e_1 is the estimation error of $\tilde{\omega}$.

According to [18], with appropriate selection of z_1, z_2, α_0 and ε_0, the observer states Z_1 and Z_2 can converge to small regions around the true values of angular velocity error $\tilde{\omega}$ and the total uncertainty $J_0^{-1}\delta$ in finite time. Denote $\sigma = \delta - J_0 Z_2$ as the estimation error of δ from the ESO (69) and (70).

Then, the command control signal u is designed as

$$u = -J_0 Z_2 - F - \alpha_1 J_0 \dot{\tilde{q}}_v - \alpha_2 J_0 \dot{\beta}(\tilde{q}_v) - k_3\zeta - \frac{1}{2}S + u_r + u_n \tag{75}$$

where u_r and u_n are as defined in (41) and (42), α_1 and α_2 are as defined in (18), and Z_2 is the real-time estimate of $x_2 = J_0^{-1}\delta$ obtained from the ESO (69) and (70).

Then, the following theorem is obtained.

Theorem 2: Consider the attitude tracking control system in (8) and (9). If Assumption 2 holds, the auxiliary system is designed as (23), the ESO is designed as (69) and (70), and the controller (75) is applied. Then, the following conclusions are obtained:

(i) The sliding mode surface S can converge into the following regions in finite time

$$S_i \leqslant \psi_i = \min\{\frac{|\sigma_i|}{\tau_1}, \left|\frac{\sigma_i}{\tau_2}\right|^{\frac{1}{\rho}}\}, \quad i = 1,2,3, \tag{76}$$

where σ_i is the i^{th} element of $\sigma = \delta - J_0 Z_2$, and τ_1, τ_2 and ρ are as defined in (41).

(ii) The tracking errors of $\tilde{q}_v$ and $\tilde{\omega}$ can converge into the following regions in finite time:

$$|\tilde{q}_i| \leqslant \vartheta_i = \max\{\eta, \min\{\frac{|\psi_i|}{\alpha_1}, \left|\frac{\psi_i}{\alpha_2}\right|^{\frac{1}{\gamma}}\}\}, \tag{77}$$

$$|\tilde{\omega}_i| \leqslant \psi_i + \alpha_1\vartheta_i + \alpha_2\vartheta_i^{\gamma}, i = 1,2,3, \tag{78}$$

where ψ_i is as defined in (76), and η, α_1, α_2 and γ are as defined in (18).

Proof: Consider the Lyapunov function candidate as

$$V = \frac{1}{2}S^T J_0 S + \frac{1}{2}\zeta^T\zeta. \tag{79}$$

Taking the derivative of (79) and substituting in the controller (75) and the auxiliary system (23) yields

$$\begin{aligned} \dot{V} &= S^T[F + u + \Delta u + \delta + \alpha_1 J_0\dot{\tilde{q}}_v + \alpha_2 J_0\dot{\beta}(\tilde{q}_v)] \\ &\quad + \zeta^T\dot{\zeta} \\ &= S^T(\delta - J_0 Z_2 + u_r - k_4\cdot\mathrm{sig}^{\gamma_1}(S) \\ &\quad - k_3\zeta - \frac{1}{2}S + \Delta u) + \zeta^T\dot{\zeta} \\ &= S^T(\delta - J_0 Z_2 + u_r) - k_4\cdot S^T\mathrm{sig}^{\gamma_1}(S) - k_3 S^T\zeta \\ &\quad - \frac{1}{2}S^T S + S^T\Delta u - k_1\zeta^T\zeta - k_2\zeta^T\mathrm{sig}^{\gamma_1}(\zeta) \\ &\quad - \left\|S^T\Delta u\right\|_1 - \frac{1}{2}\Delta u^T\Delta u + \zeta^T\Delta u \\ &\leqslant S^T(\sigma + u_r) - k_4 S^T\mathrm{sig}^{\gamma_1}(S) - k_2\zeta^T\mathrm{sig}^{\gamma_1}(\zeta) \\ &\leqslant -\mu V^{\frac{\gamma_1+1}{2}} + S^T(\sigma - \tau_1 S - \tau_2\mathrm{sig}^{\rho}(S)), \end{aligned} \tag{80}$$

where μ is as defined in (50).

Equation (80) can be rewritten as:

$$\dot{V} \leqslant -\mu V^{\frac{\gamma_1+1}{2}} - S^T[\mathrm{diag}(\tau_1 - \frac{\sigma_i}{S_i})S + \tau_2 \mathrm{sig}^{\rho}(S)], \tag{81}$$

$$\dot{V} \leqslant -\mu V^{\frac{\gamma_1+1}{2}} - S^T[\tau_1 S + \mathrm{diag}(\tau_2 - \frac{\sigma_i}{\mathrm{sgn}(S_i)|S_i|^{\rho}})\mathrm{sig}^{\rho}(S)]. \tag{82}$$

If $\mathrm{diag}(\tau_1 - \sigma_i/S_i)$ or $\mathrm{diag}(\tau_2 - \sigma_i/\mathrm{sgn}(S_i)|S_i|^{\gamma})$ are positive,

$$\dot{V} \leqslant -\mu V^{\frac{\gamma_1+1}{2}}. \tag{83}$$

Similar to the analysis process from (50) to (54) within Theorem 1, a finite-time convergence rate for the control system can be assured until $\tau_1 \leqslant |\sigma_i|/|S_i|$ and $\tau_2 \leqslant |\sigma_i|/|S_i|^{\rho}$ are all reached. Therefore, S can converge into the following regions in finite time:

$$S_i \leqslant \psi_i = \min\{\frac{|\sigma_i|}{\tau_1}, \left|\frac{\sigma_i}{\tau_2}\right|^{\frac{1}{\rho}}\}, \quad i = 1,2,3, \tag{84}$$

where $\sigma = \delta - J_0 Z_2$, and τ_1, τ_2 and ρ are as defined in (41).

Given the proof of (ii) within Theorem 1, $\tilde{q}_v$ and $\tilde{\omega}$ can converge into the following regions in finite time:

$$|\tilde{q}_i| \leqslant \vartheta_i = \max\{\eta, \min\{\frac{|\psi_i|}{\alpha_1}, \left|\frac{\psi_i}{\alpha_2}\right|^{\frac{1}{\gamma}}\}\}, \tag{85}$$

$$|\tilde{\omega}_i| \leqslant \psi_i + \alpha_1 \vartheta_i + \alpha_2 \vartheta_i^{\gamma}, i = 1,2,3. \tag{86}$$

Now (i) and (ii) have been proven.

The proof of Theorem 2 is complete. □

Remark 5: As long as the ESO parameters are properly adjusted, $\sigma = \delta - J_0 Z_2$ can converge into small regions around the origin in finite time with much smaller amplitudes than the total uncertainty δ and even the external disturbance d. As a result, the controller (75) achieves much higher control precision than controller (40), which can be verified with the simulation results.

3.3. The adaptive finite-time saturated attitude tracking controller design

The controller (40) only considers the external disturbance d and the controller (75) requires the system uncertainty being differentiable and with upper bounded first derivative which restrict the applications of the respective controllers. Hence, in order to handle more general system uncertainty which is upper bounded by a polynomial function with unknown parameters, as stated in [21,42], a continuous adaptive control procedure is introduced in this subsection. The following assumption is first introduced.

Assumption 3 [21,42]**:** The total system uncertainty δ as defined in (16) is assumed to satisfy

$$\|\delta\|_2 \leqslant c_0 + c_1\|\tilde{\omega}\|_2 + c_2\|\tilde{\omega}\|_2^2, \tag{87}$$

where c_0, c_1 and c_2 are unknown parameters and $\tilde{\omega}$ is the error angular velocity.

Remark 6: The control laws proposed in this paper are mainly based on the error angular velocity and error quaternion. Since the error quaternion satisfies the constraints of $\tilde{q}_v^T\tilde{q}_v + \tilde{q}_0^2 = 1$, and ω_d and $\dot{\omega}_d$ are also assumed to be bounded, it is reasonable to obtain [42]

$$\|u\|_2 \leqslant \varsigma_0 + \varsigma_1\|\tilde{\omega}\|_2 + \varsigma_2\|\tilde{\omega}\|_2^2, \tag{88}$$

where ς_0, ς_1 and ς_2 are unknown positive constants. Given the definition of ΔF in (14),

$$\begin{aligned}\|\Delta F\|_2 &\leqslant \|\Delta J\|_2(\|\tilde{\omega} + C\omega_d\|_2^2 \\ &\quad + \left\|\tilde{\omega}^{\times}C\omega_d - C\dot{\omega}_d\right\|_2 + \left\|\dot{\tilde{\omega}}\right\|_2) \\ &\leqslant \xi_0 + \xi_1\|\tilde{\omega}\|_2 + \xi_2\|\tilde{\omega}\|_2^2,\end{aligned} \tag{89}$$

where ξ_0, ξ_1 and ξ_2 are unknown positive constants.

Therefore, it is reasonable to have Assumption 3.

The command control signal u is designed as:

$$\begin{aligned}u = &-F - \alpha_1 J_0\dot{\tilde{q}}_v - \alpha_2 J_0\dot{\beta}(\tilde{q}_v) - k_3\zeta - \frac{1}{2}S \\ &+ u_r + u_n + u_a,\end{aligned} \tag{90}$$

$$u_a = -\hat{u}\cdot\frac{S}{\|S\|_2 + \varepsilon}, \varepsilon = \frac{k_0}{1+\hat{u}}, \tag{91}$$

$$\hat{u} = \hat{c}_0 + \hat{c}_1\|\tilde{\omega}\|_2 + \hat{c}_2\|\tilde{\omega}\|_2^2, \tag{92}$$

$$\dot{\hat{c}}_n = p_n(\|S\|_2\|\tilde{\omega}\|_2^n - \chi_n\hat{c}_n), \quad n = 0,1,2, \tag{93}$$

$$k_1 - \frac{1}{2}k_3^2 - \frac{1}{2} > 0, \tag{94}$$

where u_r and u_n are as defined in (41) and (42), α_1 and α_2 are as defined in (18), k_1 is as defined in (23), k_3, p_0, p_1, p_2, χ_0, χ_1 and χ_2 are positive constants, and $\hat{c}_0$, $\hat{c}_1$ and $\hat{c}_2$ are the real-time estimates of c_0, c_1 and c_2, respectively.

Then, the following theorem is obtained.

Theorem 3: Consider the systems in (8) and (9). If Assumption 3 holds, the auxiliary system is designed as (23) and the controller (90) is applied. Then, the following conclusions can be obtained:

(i) The sliding surface variable S can converge into the following regions in finite time:

$$|S_i| \leqslant \bar{\phi}_i = \min\{(\frac{\chi}{\tau_1})^{\frac{1}{2}}, (\frac{\chi}{\tau_2})^{\frac{1}{1+\rho}}\}, \quad i = 1,2,3, \tag{95}$$

where τ_1, τ_2 and ρ are as defined in (41), $\chi = \sum_{n=0}^{2}(\chi_n c_n^2/2 + \chi_n|c_n|^{\gamma_1+1}) + k_0,\gamma_1$, c_n, χ_n and p_n are as defined in (23), (87) and (93), and k_0 is as defined in (91).

(ii) The tracking errors of $\tilde{q}_v$ and $\tilde{\omega}$ can converge into the following regions in finite time:

$$|\tilde{q}_i| \leqslant \bar{Q}_i = \max\{\eta, \min\{\frac{|\bar{\phi}_i|}{\alpha_1}, \left|\frac{\bar{\phi}_i}{\alpha_2}\right|^{\frac{1}{\gamma}}\}\}, \tag{96}$$

$$|\tilde{\omega}_i| \leqslant \bar{\phi}_i + \alpha_1\bar{Q}_i + \alpha_2\bar{Q}_i^{\gamma}, \tag{97}$$

where $\bar{\phi}_i$ is as defined in (95), and α_1, α_2, η and γ are as defined in (18) and (20).

Proof: (i) Select the Lyapunov candidate function as

$$V = \frac{1}{2}S^T J_0 S + \frac{1}{2}\zeta^T\zeta + \frac{1}{2}\sum_{n=0}^{2}\frac{1}{p_n}\tilde{c}_n^2, \tag{98}$$

where $\tilde{c}_n = c_n - \hat{c}_n$ $(n = 0,1,2)$ are the estimation errors.

Taking the derivative of (98) and substituting in the controller (90) and the auxiliary system (23) yields

$$\begin{aligned}\dot{V} &= S^T(\delta + u_a + u_r - k_4\mathrm{sig}^{\gamma_1}(S) - k_3\zeta - \frac{1}{2}S + \Delta u)\\ &\quad + \zeta^T\dot{\zeta} - \sum_{n=0}^{2}\frac{1}{p_n}\tilde{c}_n\dot{\hat{c}}_n\\ &= S^T(\delta + u_a + u_r) - k_4 S^T\mathrm{sig}^{\gamma_1}(S) - k_3 S^T\zeta\\ &\quad - \frac{1}{2}S^TS + S^T\Delta u - k_1\zeta^T\zeta - k_2\zeta^T\mathrm{sig}^{\gamma_1}(\zeta)\\ &\quad - \left\|S^T\Delta u\right\|_1 - 0.5\Delta u^T\Delta u + \zeta^T\Delta u - \sum_{n=0}^{2}\frac{1}{p_n}\tilde{c}_n\dot{\hat{c}}_n.\end{aligned} \tag{99}$$

Then, the system becomes

$$\begin{aligned}\dot{V} &\leqslant S^T(\delta + u_a + u_r) - k_4 S^T\mathrm{sig}^{\gamma_1}(S)\\ &\quad - \zeta^T(k_1 - \frac{1}{2}k_3^2 - \frac{1}{2})\zeta\\ &\quad - k_2\zeta^T\mathrm{sig}^{\gamma_1}(\zeta) - \sum_{n=0}^{2}\frac{1}{p_n}\tilde{c}_n\dot{\hat{c}}_n\\ &\leqslant S^T(\delta + u_a + u_r) - k_4(S^TS)^{\frac{\gamma_1+1}{2}}\\ &\quad - k_2(\zeta^T\zeta)^{\frac{\gamma_1+1}{2}} - \sum_{n=0}^{2}\frac{1}{p_n}\tilde{c}_n\dot{\hat{c}}_n\\ &= S^T(\delta + u_r) - \hat{u}\cdot\frac{S^TS}{\|S\|_2 + \varepsilon} - k_4(S^TS)^{\frac{\gamma_1+1}{2}}\\ &\quad - k_2(\zeta^T\zeta)^{\frac{\gamma_1+1}{2}} - \sum_{n=0}^{2}\frac{1}{p_n}\tilde{c}_n\dot{\hat{c}}_n.\end{aligned} \tag{100}$$

The following relationship is obtained that

$$\begin{aligned}-\hat{u}\cdot\frac{S^TS}{\|S\|_2 + \varepsilon} &= -\hat{u}\|S\|_2 + (\hat{u}\varepsilon)\cdot\frac{\|S\|_2}{\|S\|_2 + \varepsilon}\\ &\leqslant -\hat{u}\|S\|_2 + k_0\cdot\frac{\hat{u}}{1+\hat{u}}\cdot\frac{\|S\|_2}{\|S\|_2 + \varepsilon},\\ &\leqslant -\hat{u}\|S\|_2 + k_0\end{aligned} \tag{101}$$

where $\hat{u}/(1+\hat{u}) < 1$ and $\|S\|_2/(\|S\|_2 + \varepsilon) < 1$ are used.

Substituting in (92) and using (101),

$$\begin{aligned}\dot{V} &\leqslant (\tilde{c}_0 + \tilde{c}_1\|\tilde{\omega}\|_2 + \tilde{c}_2\|\tilde{\omega}\|_2^2)\|S\|_2 - k_4(S^TS)^{\frac{\gamma_1+1}{2}}\\ &\quad - k_2(\zeta^T\zeta)^{\frac{\gamma_1+1}{2}} - \sum_{n=0}^{2}\frac{1}{p_n}\tilde{c}_n\dot{\hat{c}}_n + S^Tu_r + k_0.\end{aligned} \tag{102}$$

Substituting in (93), the system becomes

$$\begin{aligned}\dot{V} &\leqslant -k_4(S^TS)^{\frac{\gamma_1+1}{2}} - k_2(\zeta^T\zeta)^{\frac{\gamma_1+1}{2}}\\ &\quad + \sum_{n=0}^{2}\chi_n\tilde{c}_n\hat{c}_n + S^Tu_r\\ &= -k_4(S^TS)^{\frac{\gamma_1+1}{2}} - k_2(\zeta^T\zeta)^{\frac{\gamma_1+1}{2}}\\ &\quad - \sum_{n=0}^{2}\chi_n(\hat{c}_n - c_n)\hat{c}_n + S^Tu_r + k_0.\end{aligned} \tag{103}$$

Using $-(\hat{c}_n - c_n)\hat{c}_n \leqslant -(\hat{c}_n - \frac{c_n}{2})^2 + \frac{c_n^2}{2}$, it yields

$$\begin{aligned}\dot{V} &\leqslant -k_4(S^TS)^{\frac{\gamma_1+1}{2}} - k_2(\zeta^T\zeta)^{\frac{\gamma_1+1}{2}} + S^Tu_r\\ &\quad - \sum_{n=0}^{2}\chi_n(\hat{c}_n - \frac{c_n}{2})^2 + \sum_{n=0}^{2}\chi_n\cdot\frac{c_n^2}{2} + k_0\\ &\leqslant -k_4(S^TS)^{\frac{\gamma_1+1}{2}} - k_2(\zeta^T\zeta)^{\frac{\gamma_1+1}{2}} + S^Tu_r\\ &\quad - \sum_{n=0}^{2}\chi_n|\hat{c}_n - c_n|^{\gamma_1+1}\\ &\quad + \sum_{n=0}^{2}(\frac{\chi_n c_n^2}{2} + \chi_n|\hat{c}_n - c_n|^{\gamma_1+1}) + k_0\\ &\leqslant -k_4(S^TS)^{\frac{\gamma_1+1}{2}} - k_2(\zeta^T\zeta)^{\frac{\gamma_1+1}{2}} + S^Tu_r\\ &\quad - \sum_{n=0}^{2}\chi_n(\tilde{c}_n^2)^{\frac{\gamma_1+1}{2}}\\ &\quad + \sum_{n=0}^{2}(\frac{\chi_n c_n^2}{2} + \chi_n|c_n|^{\gamma_1+1}) + k_0\\ &\leqslant -(\frac{2}{\lambda_{\max}(J_0)})^{\frac{\gamma_1+1}{2}}\cdot k_4\cdot(\frac{1}{2}S^TJ_0S)^{\frac{\gamma_1+1}{2}}\\ &\quad - 2^{\frac{\gamma_1+1}{2}}\cdot k_2\cdot(\frac{1}{2}\zeta^T\zeta)^{\frac{\gamma_1+1}{2}} + S^Tu_r\\ &\quad - \sum_{n=0}^{2}\chi_n(2p_n)^{\frac{\gamma_1+1}{2}}(\frac{\tilde{c}_n^2}{2p_n})^{\frac{\gamma_1+1}{2}}\\ &\quad + \sum_{n=0}^{2}(\frac{\chi_n c_n^2}{2} + \chi_n|c_n|^{\gamma_1+1}) + k_0,\end{aligned} \tag{104}$$

where $\hat{c}_n \geqslant 0$ and $|\hat{c}_n - c_n| \leqslant c_n$ have been utilized based on the low pass filter characteristic of (93) and $\|S\|_2\|\tilde{\omega}\|_2^n \geqslant 0$ $(n = 0,1,2)$.

Using Lemma 2,

$$\begin{aligned}\dot{V} &\leqslant -\alpha[\frac{1}{2}S^TJ_0S + \frac{1}{2}\zeta^T\zeta + \sum_{n=0}^{2}\frac{1}{2p_n}\tilde{c}_n^2]^{\frac{\gamma_1+1}{2}}\\ &\quad - \tau_1S^TS - \tau_2S^T\mathrm{sig}^{\rho}(S) + \chi\\ &\leqslant -\alpha V^{\frac{\gamma_1+1}{2}} - \tau_1S^TS - \tau_2(S^TS)^{\frac{1+\rho}{2}} + \chi,\end{aligned} \tag{105}$$

where $\alpha = \min\{(2/\lambda_{\max}(J_0))^{(\gamma_1+1)/2}k_4,\ 2^{(\gamma_1+1)/2}k_2, \chi_0(2p_0)^{(\gamma_1+1)/2},\ \chi_1(2p_1)^{(\gamma_1+1)/2},\ \chi_2(2p_2)^{(\gamma_1+1)/2}\}$ and $\chi = \sum_{n=0}^{2}(\chi_n c_n^2/2 + \chi_n|c_n|^{\gamma_1+1}) + k_0$ are positive.

(105) can be rearranged as

$$\dot{V} \leqslant -\alpha V^{\frac{\gamma_1+1}{2}} - (\tau_1 - \frac{\chi}{S^TS})S^TS - \tau_2(S^TS)^{\frac{1+\rho}{2}}, \tag{106}$$

$$\dot{V} \leqslant -\alpha V^{\frac{\gamma_1+1}{2}} - \tau_1 S^T S - (\tau_2 - \frac{\chi}{(S^T S)^{\frac{1+\rho}{2}}})(S^T S)^{\frac{1+\rho}{2}}. \tag{107}$$

If $\tau_1 > \chi/S^T S$ or $\tau_2 > \chi/(S^T S)^{(1+\rho)/2}$ are satisfied, the convergence of S can be assured. And the convergence process will last until $\tau_1 \leqslant \chi/S^T S$ and $\tau_2 \leqslant \chi/(S^T S)^{(1+\rho)/2}$ have all been reached. Using $\tau_1 \leqslant \chi/S^T S$ and $\tau_2 \leqslant \chi/(S^T S)^{(1+\rho)/2}$, it can be obtained that $|S_i| \leqslant (\chi/\tau_1)^{1/2}$ and $|S_i| \leq (\chi/\tau_2)^{1/(1+\rho)}$ for $i = 1,2,3$, respectively. Therefore, S can converge into the following regions in finite time:

$$|S_i| \leqslant \bar{\phi}_i = \min\{(\frac{\chi}{\tau_1})^{\frac{1}{2}}, (\frac{\chi}{\tau_2})^{\frac{1}{1+\rho}}\}, i = 1,2,3, \tag{108}$$

where τ_1, τ_2 and ρ are as defined in (41), and χ is as defined in (105).

Similar to the respective parts within Theorem 1 and Theorem 2, the ultimate upper bounds of the tracking errors of $\tilde{q}_v$ and $\tilde{\omega}$ are given by

$$|\tilde{q}_i| \leqslant \bar{Q}_i = \max\{\eta, \min\{\frac{|\bar{\phi}_i|}{\alpha_1}, \left|\frac{\bar{\phi}_i}{\alpha_2}\right|^{\frac{1}{\gamma}}\}\}, \tag{109}$$

$$|\tilde{\omega}_i| \leqslant \bar{\phi}_i + \alpha_1 \bar{Q}_i + \alpha_2 \bar{Q}_i^{\gamma}, \tag{110}$$

where $\bar{\phi}_i$ is as defined in (108), and α_1, α_2, η and γ are as defined in (18) and (20).

Now (i) and (ii) have been proven.

The proof of Theorem 3 is complete. □

Remark 7: Compared with [17] and [18], Δu and δ are handled separately in this paper that the input error Δu caused by actuator saturation is compensated by the auxiliary system (23) and δ by the fast-TSM-type reaching law, ESO and the adaptive control method. In this manner, the burden of the observer can be much alleviated and the additional disturbance which comes from Δu and acts on the spacecraft can also be reduced.

Remark 8: The proposed controllers can provide finite-time convergence rate for the control systems. However, since the attracting regions are related to the system uncertainty, the precise settling time will be hard to calculate, which is the disadvantage of many TSMS-based control works, such as [11, 16–18].

Remark 9: The controller (91) is enlightened by [42], but with simplified structure, which is designed to avoid the control discontinuousness and to attenuate the input chattering within the adaptive control laws in [18–20] with only an additional k_0 introduced to the system uncertainty.

4. SIMULATIONS

Numerical simulations are conducted to verify the effectiveness of the proposed controllers. Based on the works of [15, 16, 18], the initial values of the spacecraft system are decided, including the nominal inertia J_0, the initial quaternion $q(0)$ and the initial velocity $\omega(0)$ which are as follows:

$$J_0 = [20, 1.2, 0.9; 1.2, 17, 1.4; 0.9, 1.4, 15]\text{kg}\cdot\text{m}^2,$$
$$q(0) = [0.4031, -0.2584, 0.7386, 0.4745]^T,$$
$$\omega(0) = [0,0,0]^T \text{rad/s}.$$

The inertia uncertainty is designed as:

$$\Delta J = diag\{\sin(0.1t), 2\sin(0.2t), 3\sin(0.3t)\}\text{kg}\cdot\text{m}^2.$$

The external disturbance is designed as:

$$d = 0.1 \times [\sin(0.1t), 2\cos(0.2t), 3\sin(0.3t)]^T \text{N}\cdot\text{m}.$$

The desired angular velocity is designed as:

$$\omega_d = [0.1\sin(t/40), -0.1\sin(t/50), -0.1\sin(t/60)]^T \text{ rad/s}.$$

The positive parameter a in (11) is set as $a = 0.1$.

For the purpose of comparison, three groups of simulations are undertaken under the proposed controllers in Theorem 1, Theorem 2 and Theorem 3, respectively. To make the comparison results fair and convincing, all the simulations are conducted with the same initial values defined above. The control parameters in details are shown in Table 1.

The simulation results of the controller (40) are presented in Figs. 1–4. As shown in Figs. 1–2 and 4, $\tilde{q}_v$, $\tilde{\omega}$ and S can be stabilized into small regions around the origin in finite time, with the steady states accuracy of 4×10^{-4}, 2×10^{-4} and 5×10^{-3}, respectively. Fig. 3 shows that the actual control torques can be finally limited within $\pm0.4\,\text{N}\cdot\text{m}$.

The simulation results of controller (75) are displayed in Figs. 5–8. Figs. 5–6 and 8 show the curves of $\tilde{q}_v$, $\tilde{\omega}$ and S, which can be stabilized within small regions around the origin in finite time and are finally bounded by 1×10^{-5}, 8×10^{-5} and 3×10^{-4}. Fig. 7 gives the curves of the actual control torques, which can be limited within $\pm0.4\,\text{N}\cdot\text{m}$ at last.

The simulation results of the controller (90) are shown in Figs. 9–13. Figs. 9–10 and 12 show that, $\tilde{q}_v$, $\tilde{\omega}$ and S can be stabilized in finite time which are upper bounded by 1.5×10^{-5}, 1.5×10^{-5} and 4×10^{-4} at last, respectively. In Fig. 11, the control torques can be constrained to $\pm0.4\,\text{N}\cdot\text{m}$ at last. Fig. 13 gives the curves of $\hat{c}_0$, $\hat{c}_1$ and $\hat{c}_2$, which are upper bounded.

Some key comparison results are listed in Table 2.

From the simulation results, it can be observed that:

1) From Figs. 3, 7 and 11, the actual control torques are all chattering-free and bounded within a certain range, which shows the saturation property of the proposed controllers.

Table 1. Controller parameters setting.

	Parameters Setting
Controller (40)	$\alpha_1 = 1$, $\alpha_2 = 0.5$, $\eta = 0.0001$, $\gamma = 0.6$, $\gamma_1 = 0.7$, $\rho = 0.7$, $k_1 = 2$, $k_2 = 1$, $k_3 = 0.3$, $k_4 = 1$, $\tau_1 = \tau_2 = 10$, $U_{\max} = 2\,\mathrm{N\cdot m}$, $\zeta_0 = 0.0001$.
Controller (75)	$\alpha_1 = 1$, $\alpha_2 = 0.5$, $\eta = 0.0001$, $\gamma = 0.6$, $\gamma_1 = 0.7$, $\rho = 0.7$, $k_1 = 2$, $k_2 = 1$, $k_3 = 0.3$, $k_4 = 1$, $\tau_1 = \tau_2 = 10$, $U_{\max} = 2\,\mathrm{N\cdot m}$, $\zeta_0 = 0.0001$, $z_1 = 8$, $z_2 = 0.5$, $\varepsilon_0 = 0.01$, $\alpha_0 = 0.5$.
Controller (90)	$\alpha_1 = 1$, $\alpha_2 = 0.5$, $\eta = 0.0001$, $\gamma = 0.6$, $\gamma_1 = 0.7$, $\rho = 0.7$, $k_1 = 2$, $k_2 = 1$, $k_3 = 0.3$, $k_4 = 1$, $\tau_1 = \tau_2 = 10$, $k_0 = 0.0005$, $p_0 = p_1 = p_2 = 0.1$, $\zeta_0 = 0.0001$, $\chi_0 = \chi_1 = \chi_2 = 0.001$, $U_{\max} = 2\,\mathrm{N\cdot m}$.

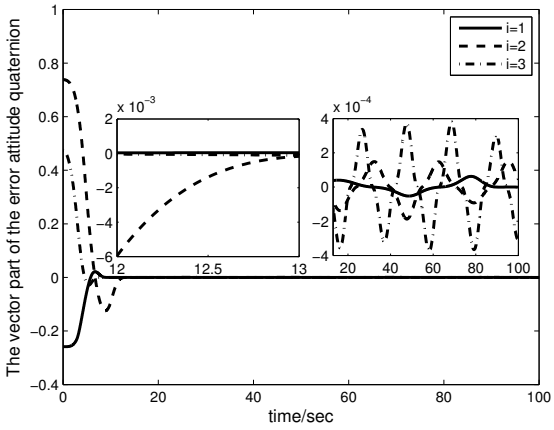

Fig. 1. The curves of $\tilde{q}_v$ under (40).

Table 2. Comparison results of the steady states accuracy.

	S	$\tilde{q}_v$	$\tilde{\omega}$
Controller (40)	5×10^{-3}	4×10^{-4}	2×10^{-4}
Controller (75)	3×10^{-4}	1×10^{-5}	8×10^{-5}
Controller (90)	4×10^{-4}	1.5×10^{-5}	1.5×10^{-5}

2) As shown by the steady states behavior in Figs. 1–2, 5–6 and 9–10, and the comparison results in Table 2, the ultimate attitude pointing accuracy and the angular velocity tracking accuracy are all stabilized within satisfactory ranges even with the system uncertainty and control input constraint, which shows that the attitude tracking control missions have been successfully accomplished by the proposed control methods.

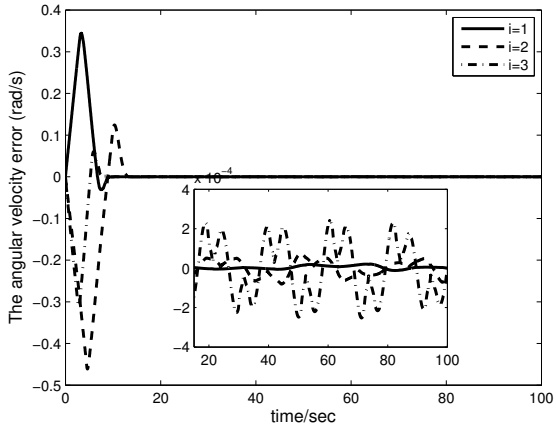

Fig. 2. The curves of $\tilde{\omega}$ under (40).

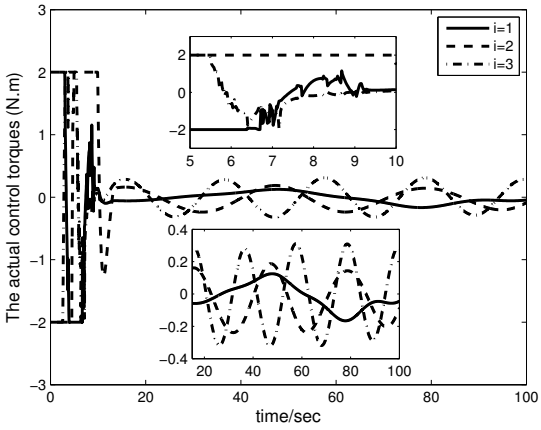

Fig. 3. The actual control torques $\mathrm{sat}(u)$ under (40).

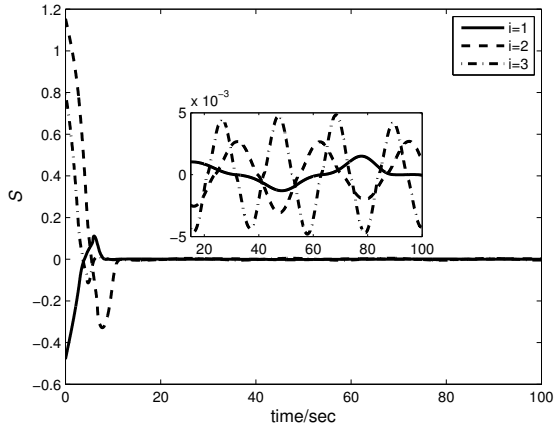

Fig. 4. The curves of S under (40).

3) The last two group simulations achieve much higher control precision. With the help of the ESO as defined in (69) and (70), and the adaptive law as defined in

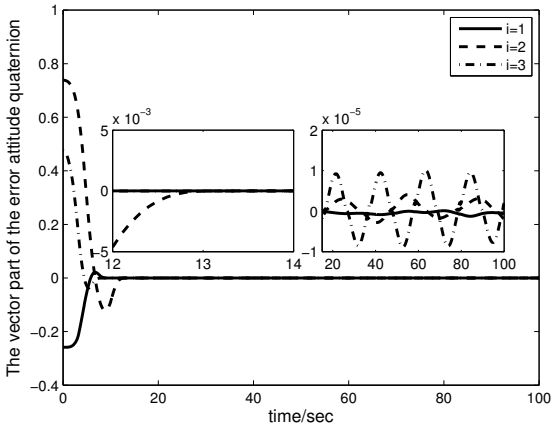

Fig. 5. The curves of $\tilde{q}_v$ under (75).

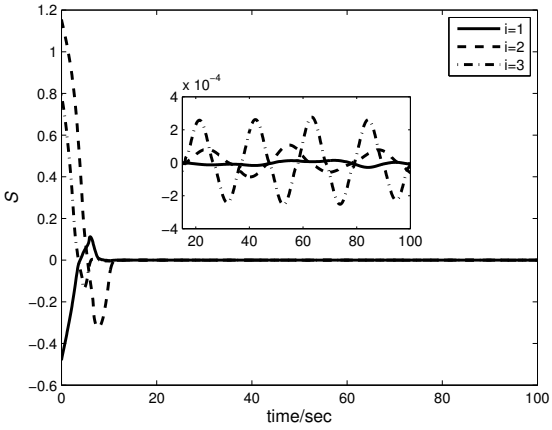

Fig. 8. The curves of S under (75).

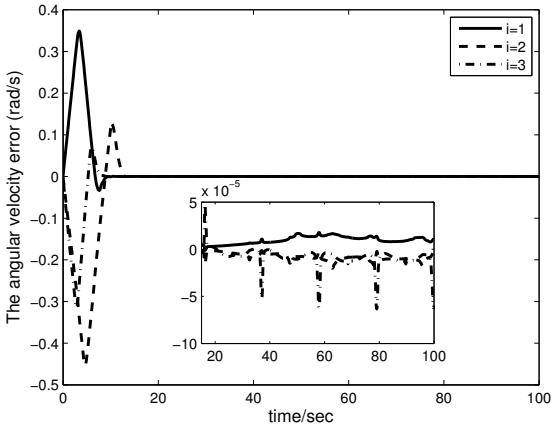

Fig. 6. The curves of $\tilde{\omega}$ under (75).

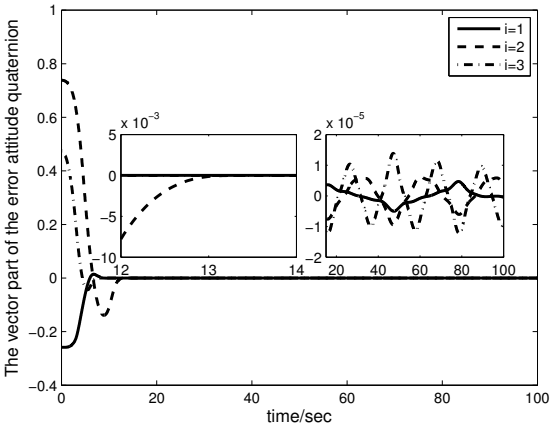

Fig. 9. The curves of $\tilde{q}_v$ under (90).

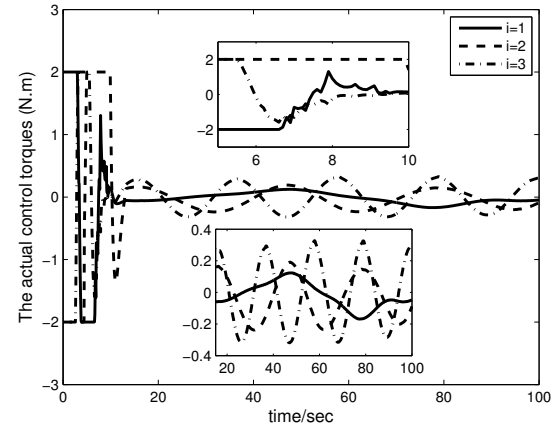

Fig. 7. The actual control torques under (75).

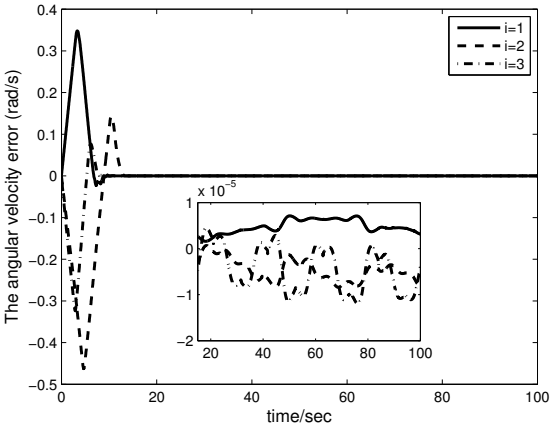

Fig. 10. The curves of $\tilde{\omega}$ under (90).

(91), the total system uncertainty under the respective controllers can be compensated to have a much smaller amplitude, as a result higher control precisions are obtained.

5. CONCLUSION

In this paper, we research the finite-time attitude tracking control problem of rigid spacecraft under inertia un-

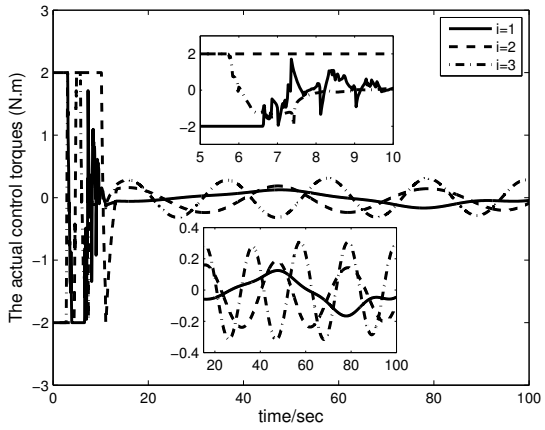

Fig. 11. The actual control torques under (90).

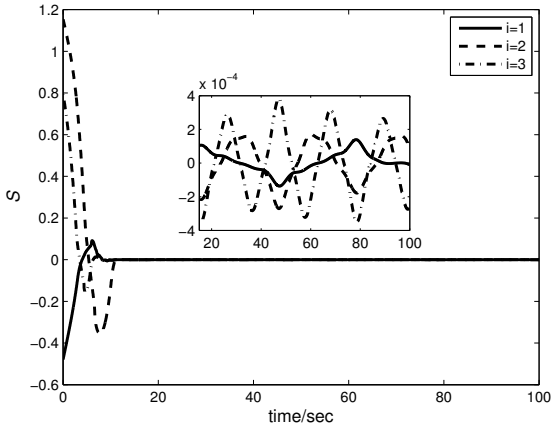

Fig. 12. The curves of S under (90).

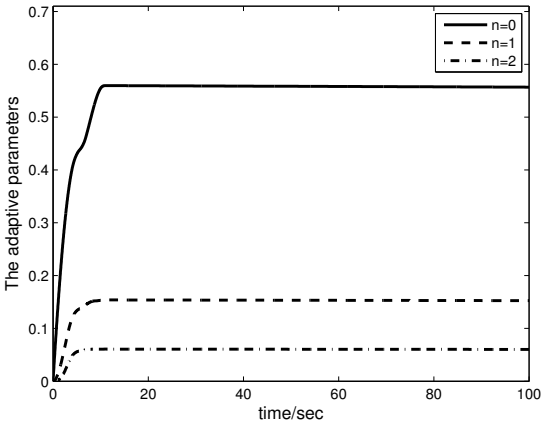

Fig. 13. The curves of the adaptive parameters.

certainty, external disturbance and actuator saturation with three different controllers designed. Benefits of the proposed controllers include finite-time convergence, attenuated input chattering and robustness with respect to model uncertainty, external disturbance and actuator saturation. The stability of the resultant closed-loop systems has been proved through the Lyapunov stability theory. Simulations are undertaken to show the effectiveness of the proposed controllers.

REFERENCES

[1] W. C. Luo, Y. C. Chu, and K. V. Ling, "H-infinity inverse optimal attitude-tracking control of rigid spacecraft," *Journal of Guidance Control & Dynamics*, vol. 28, no. 3, pp. 481-494, 2005.

[2] J. R. Forbes, "Passivity-based attitude control on the special orthogonal group of rigid-body rotations," *Journal of Guidance Control & Dynamics*, vol. 36, no. 6, pp. 1596-1605, 2013. [click]

[3] S. Sheng and C. Sun, "An adaptive attitude tracking control approach for an unmanned helicopter with parametric uncertainties and measurement noises," *International Journal of Control, Automation and Systems*, vol. 14, no. 1, pp. 217-228, 2016. [click]

[4] R. Kristiansen, P. J. Nicklasson, and J. T. Gravdahl, "Satellite attitude tracking by quaternion-based backstepping," *IEEE Transactions on Control Systems Technology*, vol. 17, no. 1, pp. 227-232, 2009. [click]

[5] Y. J. Liu and S. Tong, "Optimal control-based adaptive NN design for a class of nonlinear discrete-time block triangular systems," *IEEE Transactions on Cybernetics*, vol. 46, no. 11, pp. 2670-2680, 2016. [click]

[6] J. K. Lee, Y. H. Choi, and B. P. Jin, "Sliding mode tracking control of mobile robots with approach angle in Cartesian coordinates," *International Journal of Control, Automation and Systems*, vol. 13, no. 3, pp. 718-724, 2015. [click]

[7] Y. J. Liu and S. Tong, "Barrier Lyapunov functions for Nussbaum gain adaptive control of full state constrained nonlinear systems," *Automatica*, vol. 76, pp. 143-152, 2017.

[8] S. T. Venkataraman and S. Gulati, "Control of nonlinear systems using terminal sliding modes," *American Control Conference*, vol. 115, no. 3, pp. 891-893, 2009.

[9] Y. Tang, "Terminal sliding mode control for rigid robots," *Automatica*, vol. 34, no. 1, pp. 51-56, 1998.

[10] E. Jin and Z. Sun, "Robust controllers design with finite time convergence for rigid spacecraft attitude tracking control," *Aerospace Science & Technology*, vol. 12, no. 4, pp. 324-330, 2008.

[11] S. Yu, X. Yu, B. Shirinzadeh, and Z. Man, "Continuous finite time control for robotic manipulators with terminal sliding mode," *Automatica*, vol. 41, no. 11, pp. 1957-1964, 2005. [click]

[12] K. Lu and Y. Xia, "Finite-time fault-tolerant control for rigid spacecraft with actuator saturations," *IET Control Theory & Applications*, vol. 7, no. 11, pp. 1529-1539, 2013. [click]

[13] P. M. Tiwari, S. Janardhanan, and M. U. Nabi, "A finite-time convergent continuous time sliding mode controller for spacecraft attitude control," *International Workshop on Variable Structure Systems*, pp. 399-403, 2010.

[14] S. Wu, G. Radice, Y. Gao, and Z. Sun, "Quaternion-based finite time control for spacecraft attitude tracking," *Acta Astronautica*, vol. 69, no. 1-2, pp. 48-58, 2011. [click]

[15] Y. Guo, S. M. Song, and X. H. Li, "Quaternion-based finite-time control for attitude tracking of the spacecraft without unwinding," *International Journal of Control, Automation and Systems*, vol. 13, no. 6, pp. 1351-1359, 2015. [click]

[16] C. Pukdeboon and P. Siricharuanun, "Nonsingular terminal sliding mode based finite-time control for spacecraft attitude tracking," *International Journal of Control, Automation and Systems*, vol. 12, no. 3, pp. 530-540, 2014. [click]

[17] Q. Hu, B. Li, and J. Qi, "Disturbance observer based finite-time attitude control for rigid spacecraft under input saturation," *Aerospace Science & Technology*, vol. 39, pp. 13-21, 2014.

[18] K. Lu, Y. Xia, and M. Fu, "Controller design for rigid spacecraft attitude tracking with actuator saturation," *Information Sciences*, vol. 220, no. 220, pp. 343-366, 2013.

[19] Z. Zhu, Y. Xia, and M. Fu, "Attitude stabilization of rigid spacecraft with finite-time convergence," *International Journal of Robust & Nonlinear Control*, vol. 21, no. 6, pp. 686-702, 2011.

[20] Z. Song, H. Li, and K. Sun, "Finite-time control for nonlinear spacecraft attitude based on terminal sliding mode technique," *ISA Transactions*, vol. 53, no. 1, pp. 117-124, 2014.

[21] K. Lu and Y. Xia, "Adaptive attitude tracking control for rigid spacecraft with finite-time convergence," *Automatica*, vol. 49, no. 12, pp. 3591-3599, 2013. [click]

[22] A. H. J. D. Ruiter, "Adaptive spacecraft attitude control with actuator saturation," *Journal of Guidance Control & Dynamics*, vol. 33, no. 5, pp. 1692-1696, 2012. [click]

[23] Y. J. Liu, S. Tong, D. J. Li and Y. Gao, "Fuzzy adaptive control with state observer for a Class of nonlinear discrete-time systems with input constraint," *IEEE Transactions on Fuzzy Systems*, vol. 24, no. 5, pp. 1147-1158, 2015. [click]

[24] L. Wang, T. Chai, and L. Zhai, "Neural-network-based terminal sliding mode control of robotic manipulators including actuator dynamics," *IEEE Transactions on Industrial Electronics*, vol. 56, no. 9, pp. 3296-3304, 2009. [click]

[25] A. M. Zou, K. D. Kumar, Z. G. Hou, and X. Liu, "Finite-time attitude tracking control for spacecraft using terminal sliding mode and Chebyshev neural network," *IEEE Transactions on Systems Man & Cybernetics, Part B, Cybernetics*, vol. 41, no. 4, pp. 950-963, 2011.

[26] Y. J. Liu, S. Tong, C. L. Chen and D. J. Li, "Neural controller design based adaptive control for nonlinear MIMO systems with unknown hysteresis inputs," *IEEE Transactions on Cybernetics*, vol. 46, no. 1, pp. 9-19, 2016.

[27] C. L. Chen, G. X. Wen, Y. J. Liu, and Z. Liu, "Observer-based adaptive backstepping consensus tracking control for high order nonlinear semi-strict-feedback multiagent systems," *IEEE Transactions on Cybernetics*, vol. 46, no. 7, pp. 1591-1601, 2016.

[28] C. L. P. Chen, Y. J. Liu, and G. X. Wen, "Fuzzy neural network based adaptive control for a class of uncertain nonlinear stochastic systems," *IEEE Transactions on Cybernetics*, vol. 44, no. 5, pp. 583-593, 2014. [click]

[29] G. X. Wen, C. L. P. Chen, Y. J. Liu, and Z. Liu, "Neural-network-based adaptive leader-following consensus control for second-order non-linear multi-agent systems," *IET Control Theory and Applications*, vol. 9, no. 13, pp. 1927-1934, 2015. [click]

[30] J. D. Boskovic, S. M. Li, and R. K. Mehra, "Robust tracking control design for spacecraft under control input saturation," *Journal of Guidance Control & Dynamics*, vol. 27, no. 4, pp. 627-633, 2004. [click]

[31] R. J. Wallsgrove and M. R. Akella, "Globally stabilizing saturated attitude control in the presence of bounded unknown disturbances," *Journal of Guidance Control & Dynamics*, vol. 28, no. 5, pp. 957-963, 2005. [click]

[32] M. R. Akella, A. Valdivia, and G. R. Kotamraju, "Velocity-free attitude controllers subject to actuator magnitude and rate saturations," *Journal of Guidance Control & Dynamics*, vol. 28, no. 4, pp. 659-666, 2005. [click]

[33] D. Bustan, N. Pariz, and S. K. Sani, "Robust fault-tolerant tracking control design for spacecraft under control input saturation," *ISA Transactions*, vol. 53, no. 4, pp. 1073-1080, 2014. [click]

[34] A. M. Zou, K. D. Kumar, and A. H. J. D. Ruiter, "Robust attitude tracking control of spacecraft under control input magnitude and rate saturations," *International Journal of Robust & Nonlinear Control*, no. 26, pp. 799-815, 2016.

[35] J. Hu and H. Zhang, "A simple saturated control framework for spacecraft with bounded disturbances," *International Journal of Robust & Nonlinear Control*, vol. 26, no. 3, pp. 367-384, 2015.

[36] Haibo Du and Shihua Li. "Finite-time attitude stabilization for a spacecraft using homogeneous method," *Journal of Guidance Control & Dynamics*, vol. 35, no. 3, pp. 740-748, 2012. [click]

[37] Q. Hu, J. Zhang, and M. I. Friswell, "Finite-time coordinated attitude control for spacecraft formation flying under input saturation," *Journal of Dynamic Systems Measurement & Control*, vol. 137, no. 6, 2015.

[38] B. Xiao, Q. Hu, and M. I. Friswell, "Active fault-tolerant attitude control for flexible spacecraft with loss of actuator effectiveness," *International Journal of Adaptive Control & Signal Processing*, vol. 27, no. 11, pp. 925-943, 2013. [click]

[39] J. Ma, P. Li, L. Geng, and Z. Zheng, "Adaptive finite-time attitude tracking control of an uncertain spacecraft with input saturation," *IEEE Conference on Control Application (CAA), Part of 2015 IEEE Multi-Conference on Systems and Control*, Sydney, Australia, pp. 930-935, 2015.

[40] M. D. Shuster, "A survey of attitude representations," *The journal of the Astronautical Sciences*, vol. 41, no. 4, pp. 439-517, 1993.

[41] D. J. Zhao and D. G. Yang, "Model-free control of quadrotor vehicle via finite-time convergent extended state observer," *International Journal of Control, Automation and Systems*, vol. 14, no. 1, pp. 242-254, 2016. [click]

[42] W. C. Cai, X. H. Liao, and Y. D. Song, "Indirect robust adaptive fault-tolerant control for attitude tracking of spacecraft," *Journal of Guidance Control & Dynamics*, vol. 31, no. 5, pp. 1456-1463, 2008. [click]

Hai-Tao Chen received his B.S. and M.S. degrees in School of Automation from USTB. Currently, he is a Ph.D. student in the School of Astronautics at Harbin Institute of Technology. His main research interests include spacecraft attitude control, sliding mode control and adaptive control.

Shen-Min Song received his Ph.D. degree in Control Theory and Application from Harbin Institute of Technology in 1996. He carried out postdoctoral research at Tokyo University from 2000 to 2002. He is currently a professor in the School of Astronautics at Harbin Institute of Technology. His main research interests include spacecraft guidance and control, intelligent control, and nonlinear theory and application.

Zhi-Bin Zhu received his Ph.D. degree in Control Science and Engineering from Harbin Institute of Technology in 2009. He is currently a senior engineer at Beijing Institute of Control Engineering. His main research interests include nonlinear control, spacecraft guidance and control, space robot on-orbit control.